

Limb Sensing, on the Path to Better Weather Forecasting

Poster: A43H-2573

AGU Fall Meeting

**Larry L. Gordley, Tom Marshall,
Dave Fritts --- GATS**

**John Fisher --- Brandywine
Photonics**



Global Atmospheric Technologies and Sciences



ABSTRACT

Earth limb observation from orbiting sensors has a rich history. The cold space background, long optical paths, and limb geometry provide formidable advantages for calibration, sensitivity and retrieval of vertically well-resolved geophysical parameters. The measurement of limb refraction provides temperature and pressure profiles unburdened by spectral calibration or gas concentration knowledge, leading to reliable long-term trends. This talk discusses those advantages and our relevant achievements with data from the SOFIE instrument on the AIM satellite. In the process we describe a path to advances in calibration, sensitivity, profile fidelity, and synergy between limb sensors and nadir sounders. These advances include small-sat compatible size, elimination of on-board calibration systems and simple static designs, dramatically reducing risk, complexity and cost. We submit that these advances, made possible by modern ADCS, FPS, GPS and new optical capabilities, will lead to improvements in weather forecasting and climate observation.

Keywords: Remote Sensing, Satellite, Atmospheric Dynamics, Earth Limb

Three Types of Measurements – Four Sensors

All are small static, passive simple instruments

RAP (Refraction Angle Profiling) – T and P from surface to mid stratosphere from limb measurements. Two sources:

GPSRO (Global Positioning Systems Radio Occultation)

TStar (Temperature from imaging Star field occultation)

DSGF (Doppler Scanning with Gas Filters) – Emission imaging through a gas filter. Suggested by Curtis et al. 1974. Two multi-channel (multi-image) instrument:

DWTS (Doppler Wind and Temperature Sounder) - **Limb** DSGF that profiles wind and temperature from 20 to 200 km. (Gordley, 2011)

HATS (High Altitude Temperature Sounder) - **Nadir** DSGF that profiles temperature from cloud-top to 100 km given **LCER** CO₂ and T, P results.

TEI (Thermal Emission Imaging)

LCER (**Limb** CO₂ Emission Radiometer)

Given **TStar** and **DWTS** T,P, results, provides CO₂ concentration.

Given CO₂ concentration, provides T, P from cloud-top to 100 km.

Atmospheric Coupling

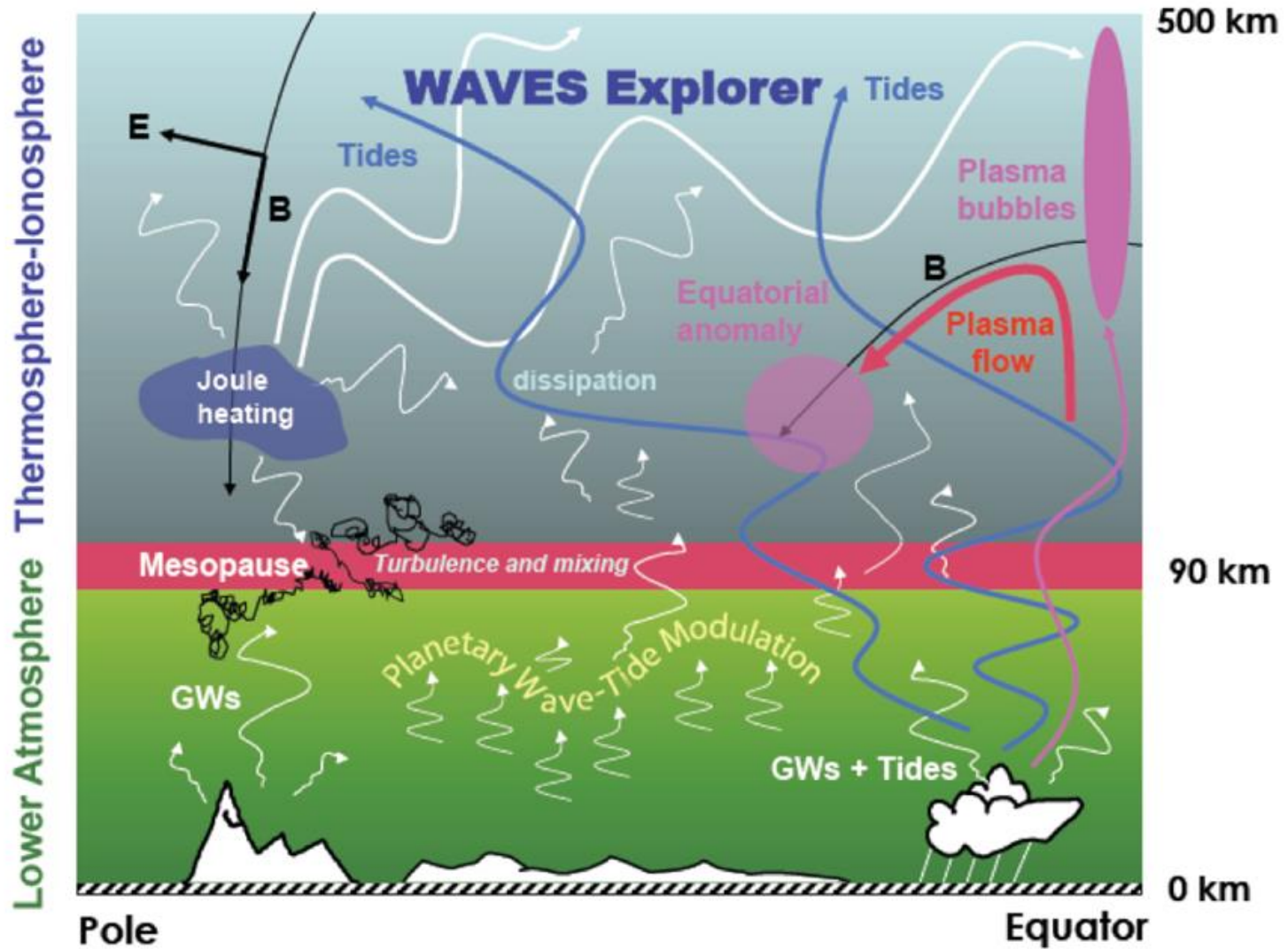


Figure 1. Lower atmosphere is continuously modulating the upper atmosphere. Observing and understanding that coupling will add to our forecasting skill.

Observation of Upper Atmosphere Dynamics

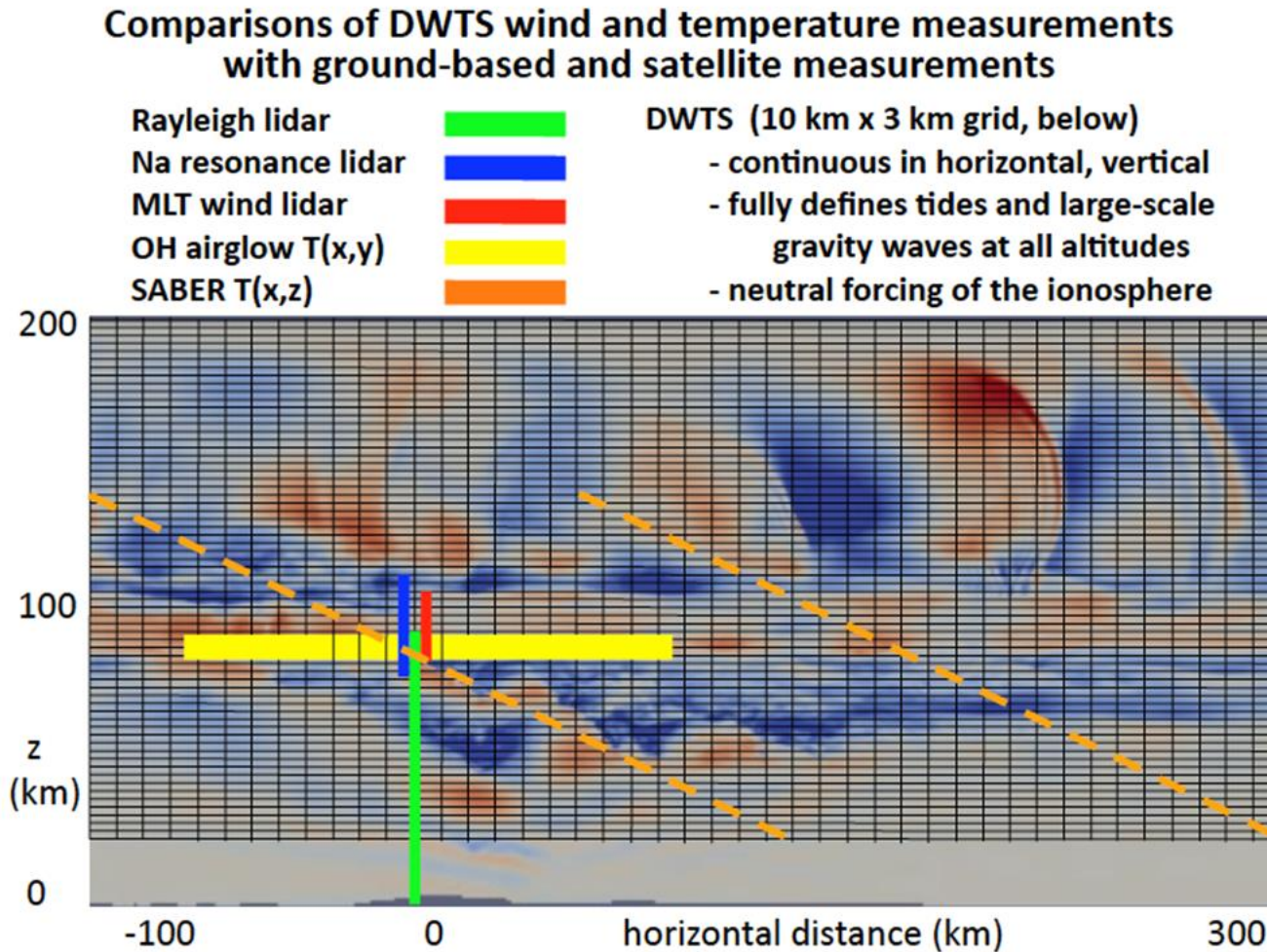


Figure 2. Color contour depicts zonal wind speed over Andes generated by surface level winds. It is unresolvable by current technology. DWTS would fill that void.

CUAD Geometry

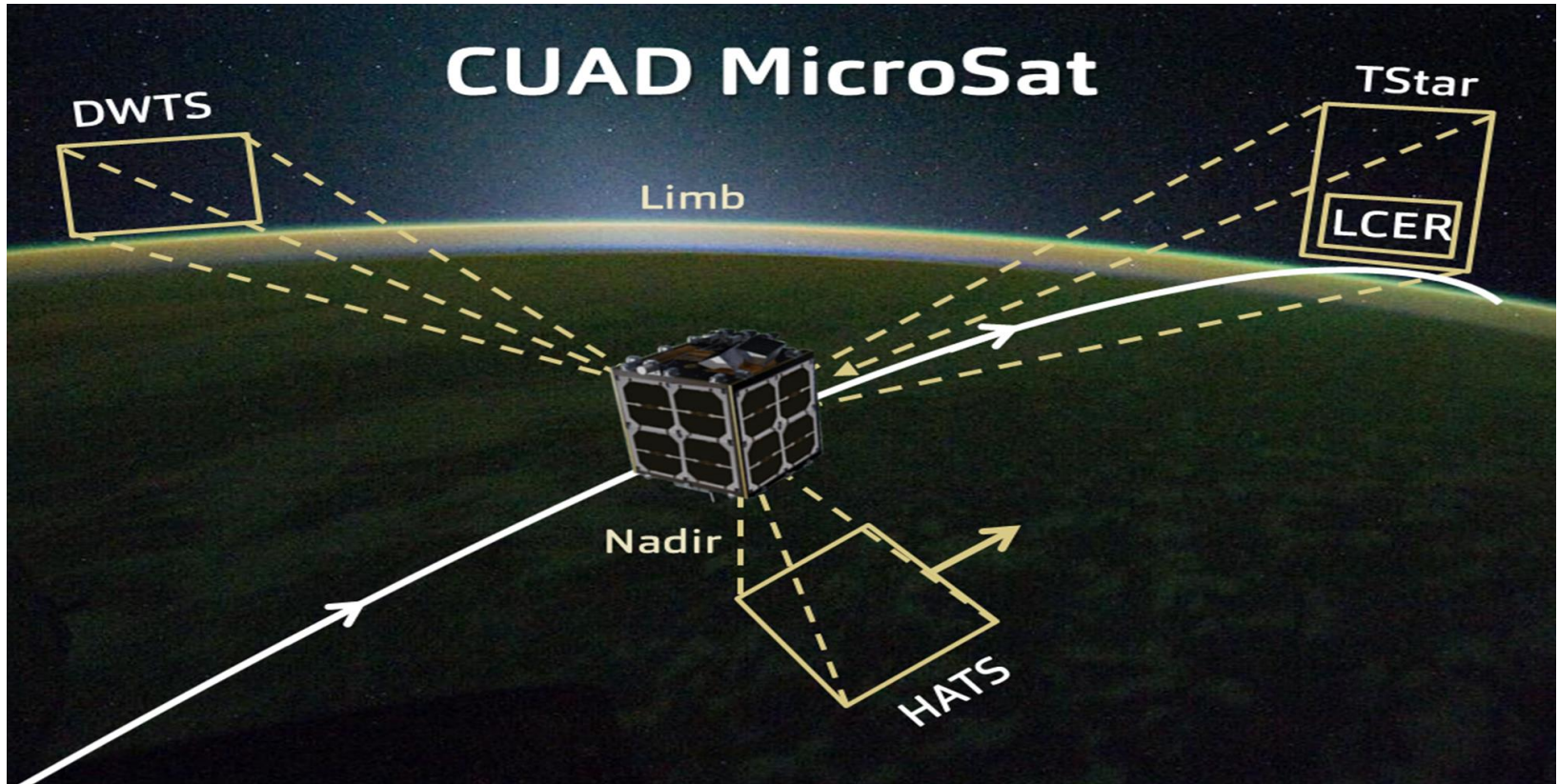


Figure 3. Viewing geometry of the 4 static imagers employed by the CUAD (Constellation for Upper Atmosphere Dynamics) system. The system requires no onboard scanning or calibration system

Lunar Example of Limb Image Refraction Effects



Figure 5. Tracking celestial bodies during occultation enables the inference of refraction angle profiles that can be converted to very accurate temperature and pressure profiles. This technique is operational on the SOFIE project. (Gordley 2009)

Temperature accuracy and precision from SOFIE Refraction angle measurements

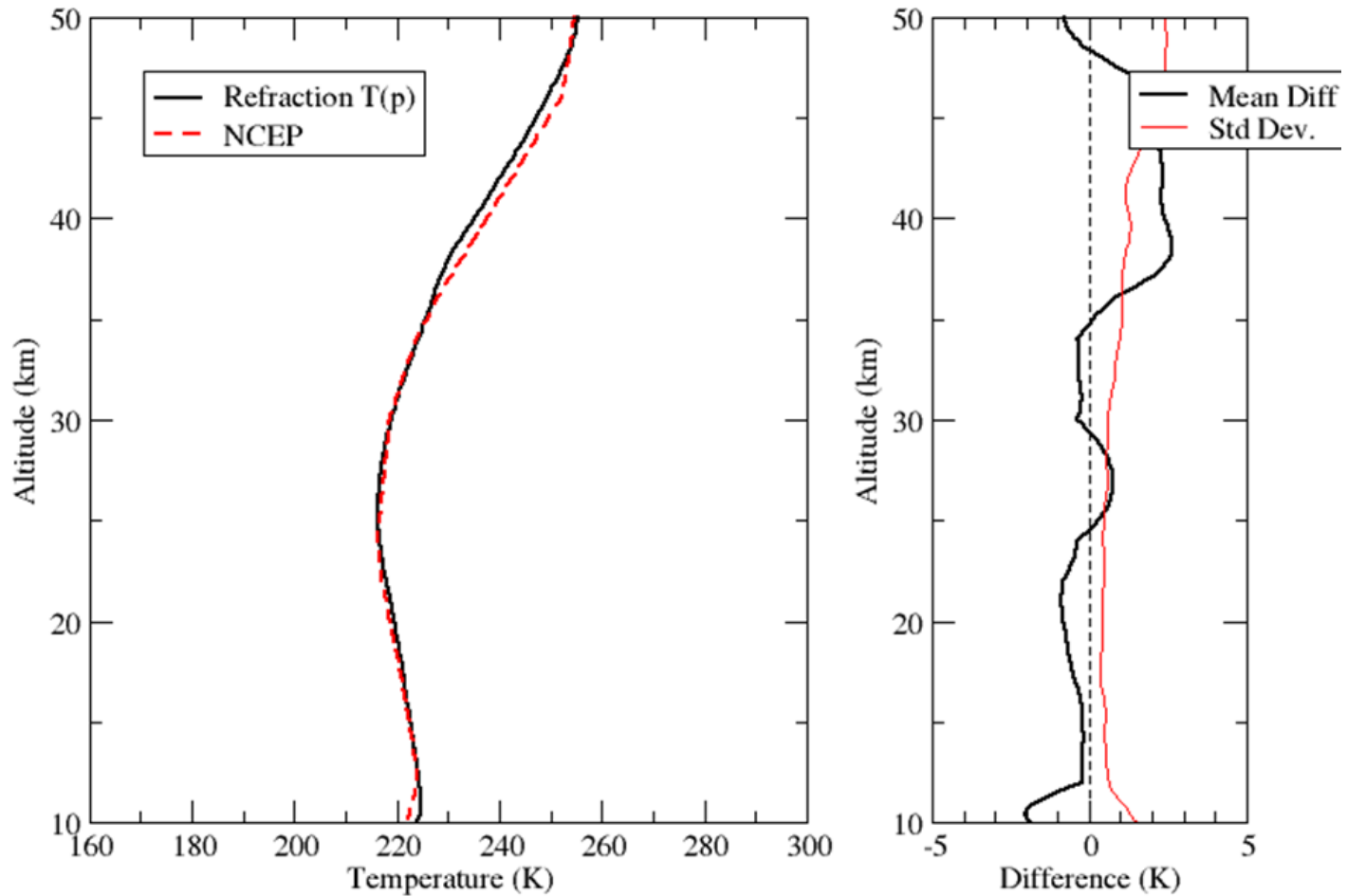


Figure 6. Typical statistical accuracy of temperature retrievals from the inversion of SOFIE refraction profile measurements.

Occulting Star Field Simulation

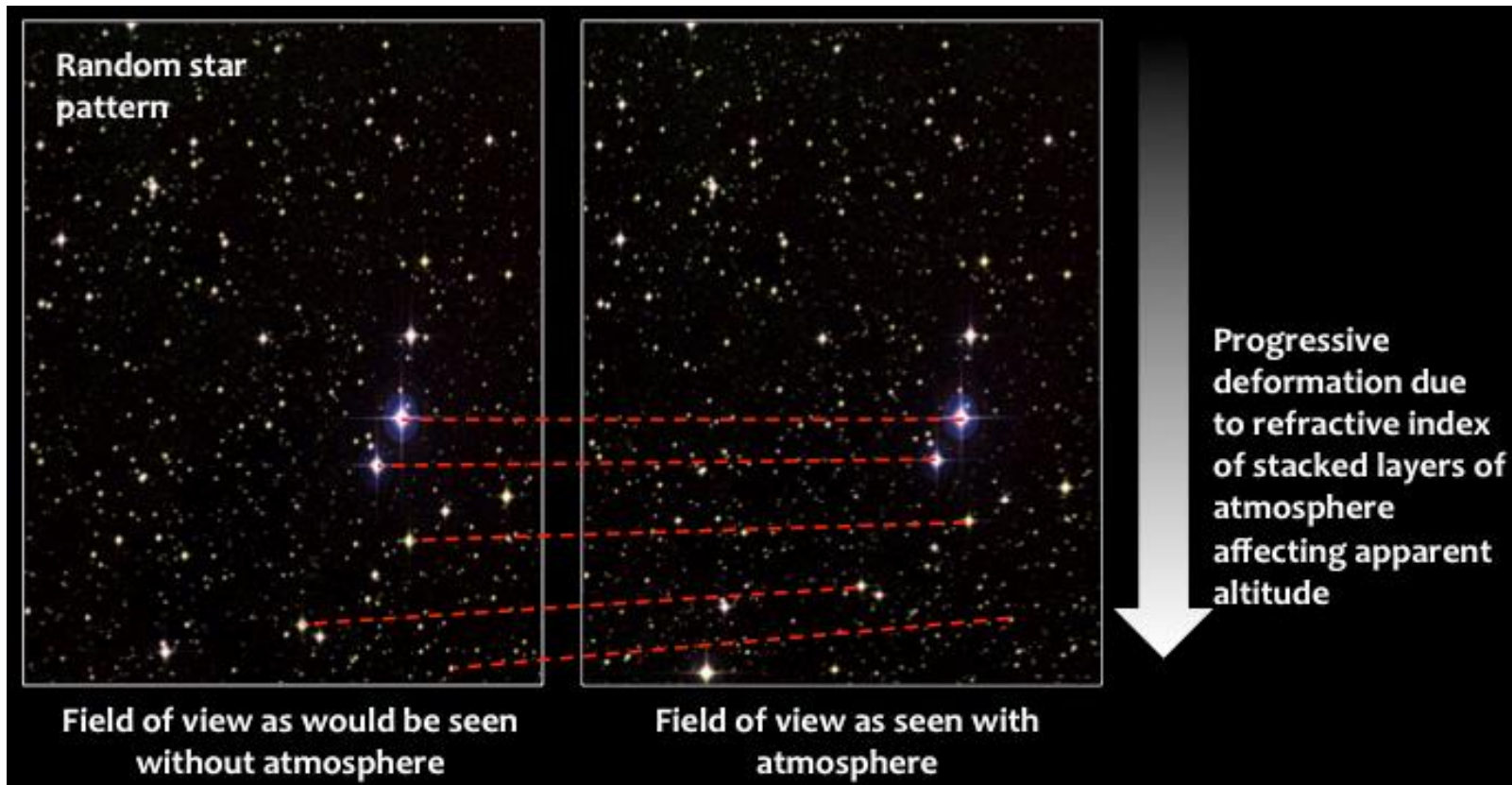


Figure 7. Refraction profiles can be derived from occulting star fields by horizontally integrating the images, then measuring the contraction of the image as a function of angle. **Tstar** is based on this concept.

Generic Imager

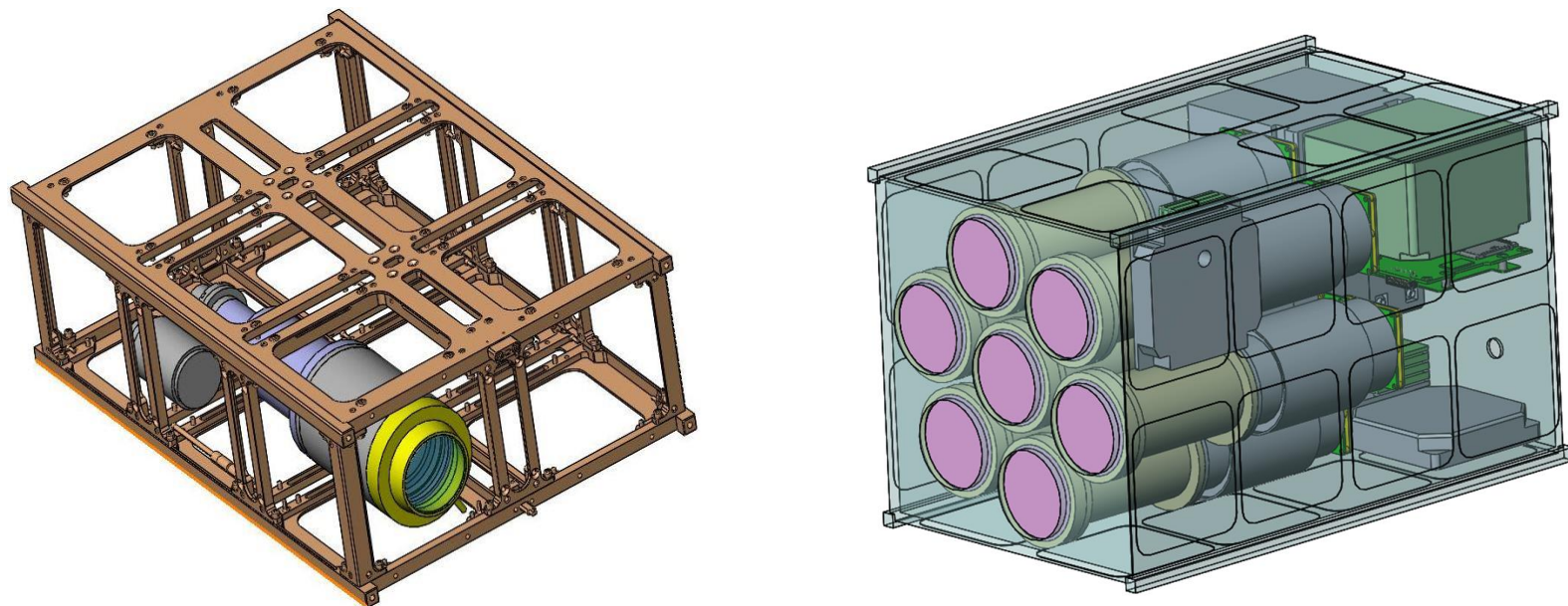


Figure 8. Every instrument in the CUAD system is a simple small imaging instrument like that depicted on left, with or without a gas cell in front of the aperture. The instrument concept on the right is for a 7-channel downward looking DSGF instrument we call **HATS** (High altitude thermal sounder (a 16 U design)).

DSGF The DWTS example

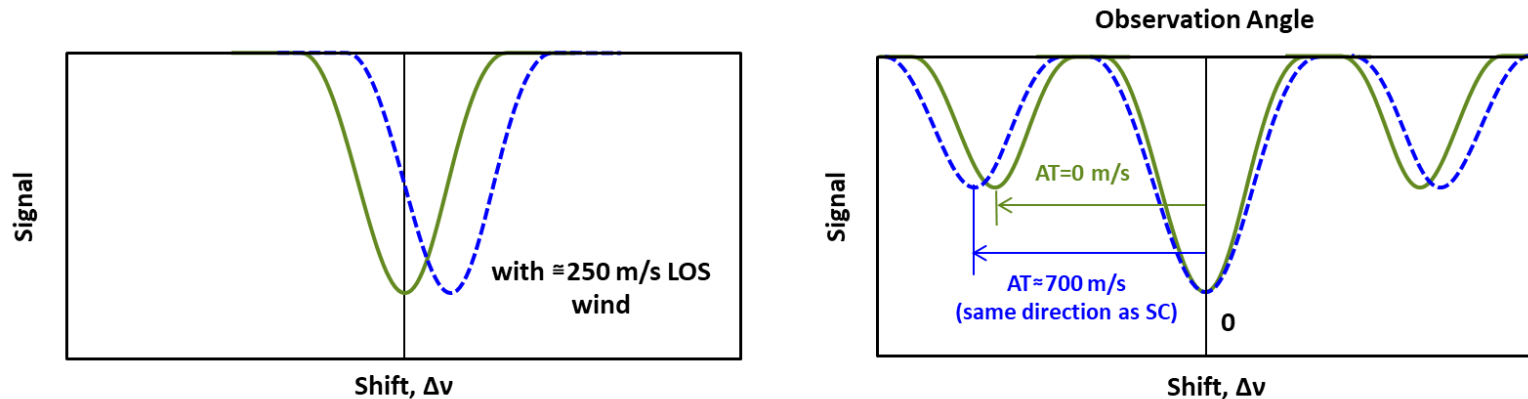


Figure 9. Example of the signal from a **DWTS** instrument. The left depicts an along-sight wind effect. The right depicts an along-track wind effect for a gas with splitting from lambda doubling (in this case nitric oxide). Temperature can also be inferred from the width of the signal dip feature. See Gordley 2011.

DWTS Error Estimates

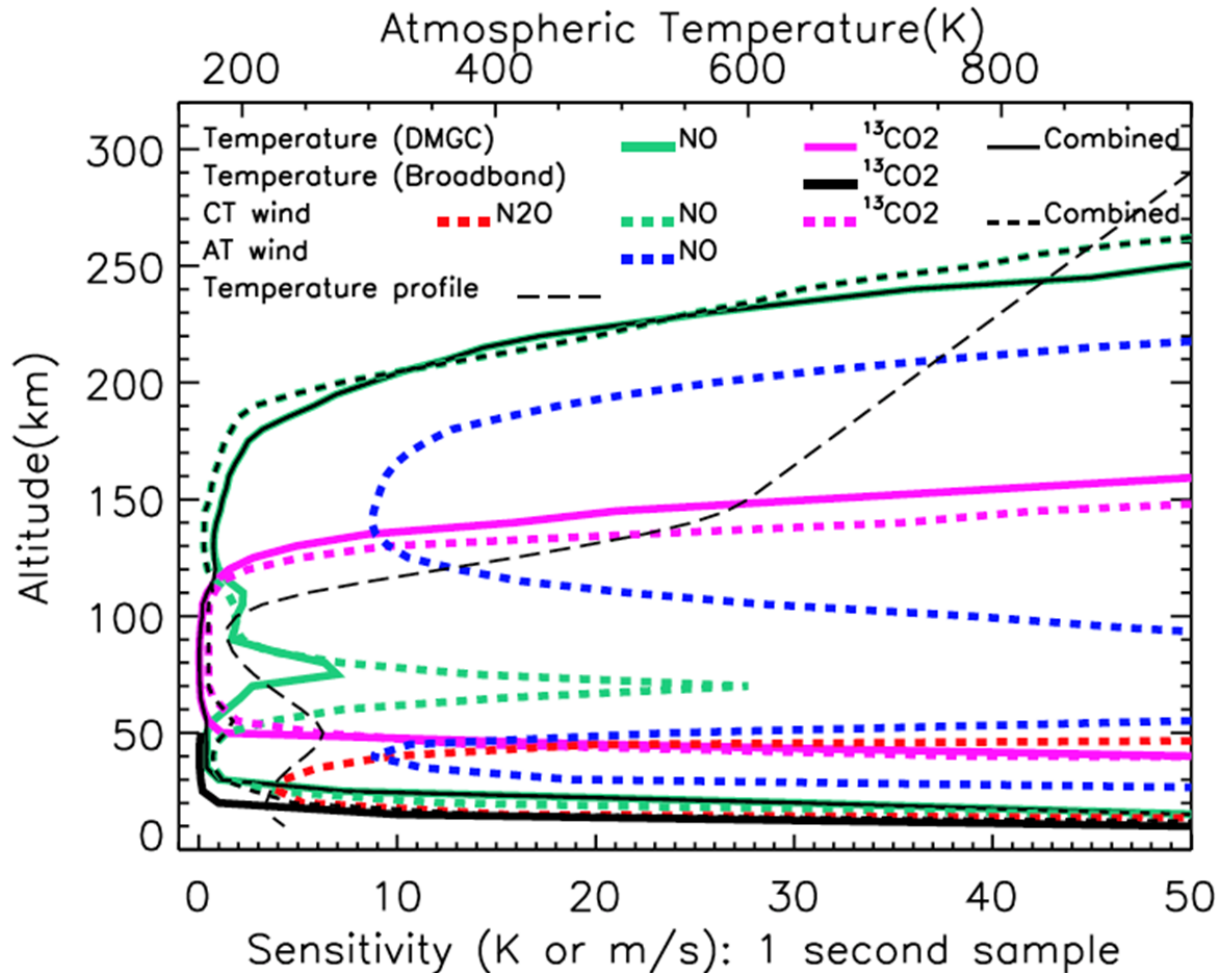


Figure 10. Error estimates for a 3-channel DWTS instrument. See Gordley 2011

HATS Averaging Kernels

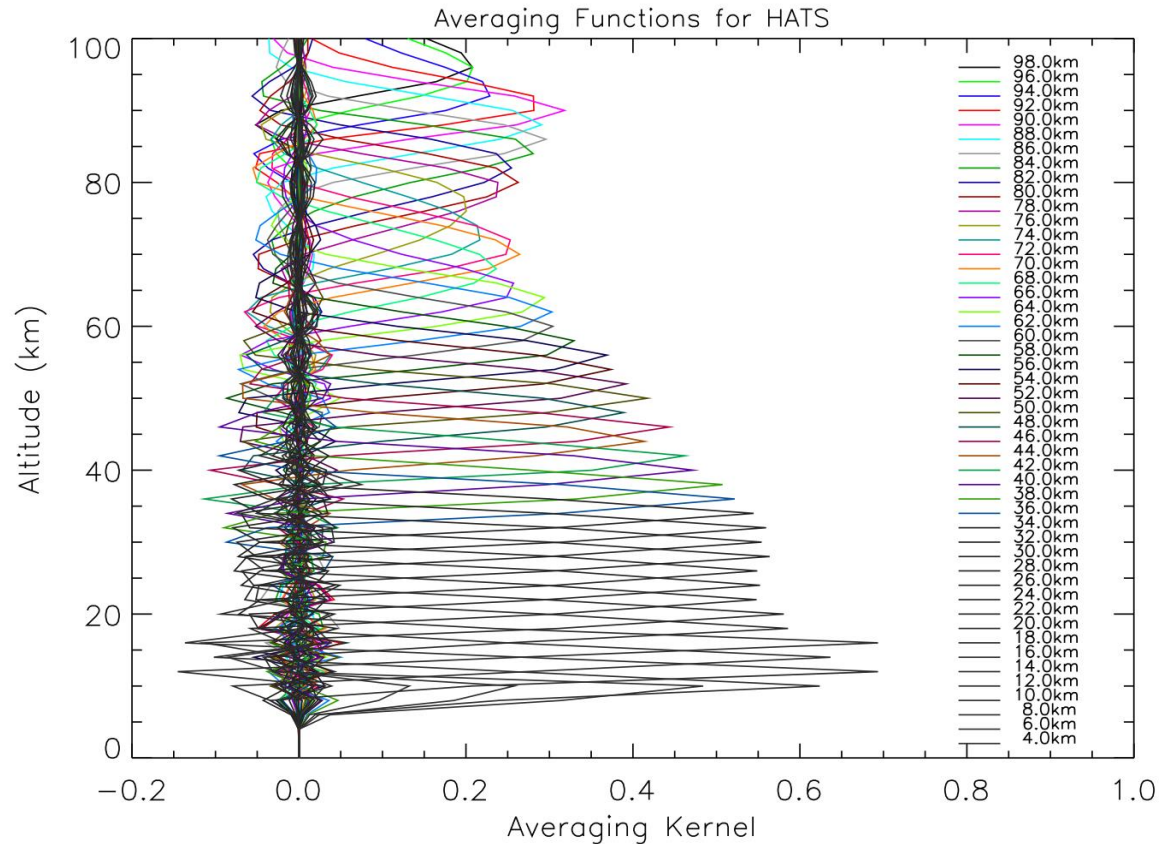


Figure 11. Averaging kernels possible with a 7-channel DSGF instrument called **HATS. These were created with a variety of $\frac{1}{2}$ % filters placed throughout the spectral region shown in figure 12.**

CO₂ Mean Emission Altitude

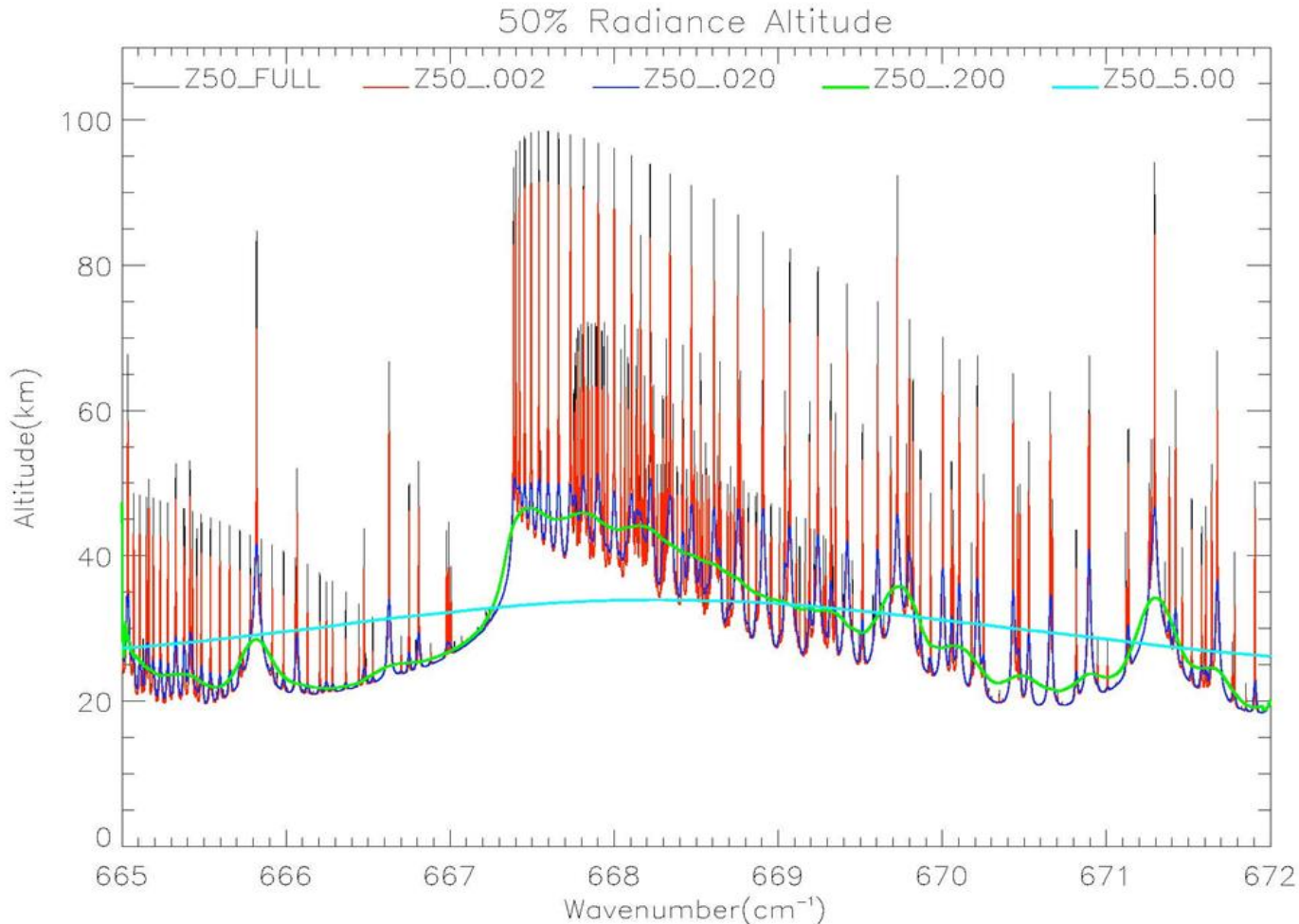


Figure 12. Mean altitude of emission measured with instruments of various spectral resolution. Demonstrates altitude information to 100km is possible.

HATS Profile Retrieval Example

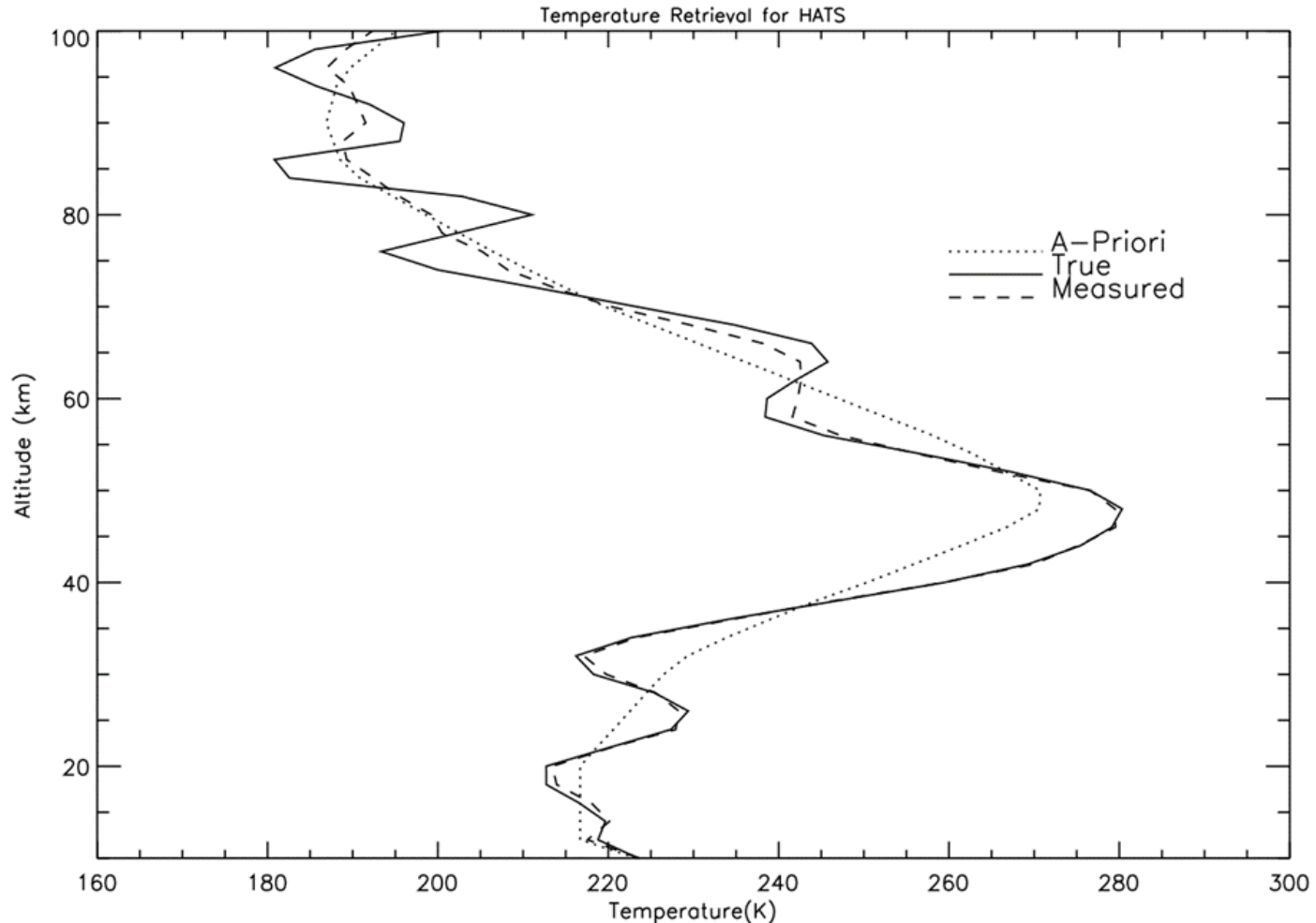


Figure 13. Typical **HATS** temperature retrieval using an optimal estimation approach following Rogers. The a priori is the limb T retrieval supplied by the **LCER** measurements.

In Summary

Earth Limb measurements enable the observation, of Upper Atmosphere Dynamics -Temperature and Wind- with small static imagers and vicarious calibration schemes. These observations have sufficient vertical and horizontal resolution to fully characterize the impact of gravity waves on the upper atmosphere. Modern technological advances in ADCS, FPAs, Cooling, Power AR coating, plus a measurement technique called Doppler Scanning with Gas Filters (DSGF), make it possible.

References

1. Gordley, L. L., Benjamin T. Marshall, "Doppler Wind and Temperature Sounder: A new approach using gas filter correlation radiometry", JARS, Vol 5, 2011.
2. Gordley, L. L., John Burton, Benjamin T. Marshall, Martin McHugh, Lance Deaver, Joel Nelsen, James M. Russell, and Scott Bailey, "High precision refraction measurements by solar imaging during occultation: results from SOFIE," Appl. Opt., 48, 4814-4825, 2009.
3. Gordley, L. L., Earl Thompson, Martin McHugh, Ellis Remsberg, James Russell III and Brian Magill, "Accuracy of atmospheric trends inferred from the Halogen Occultation Experiment data", J. Appl. Remote Sens. 3, 033526 (Apr 20, 2009).
4. Russell, J. M. III, L. L. Gordley, J. H. Park, S. R. Drayson, W. D. Hesketh, R. J. Cicerone, A. F. Tuck, J. E. Fredrick, J. E. Harries, and P. J. Crutzen, "The Halogen Occultation Experiment," J. Geophys. Res. 98 (10), 777-10797 (1993).
5. P.D. Curtis, J.T. Houghton, G.D. Peskett and C.D. Rodgers, Pro. R. Soc. Lond. A 1974 337, 135-150. doi: 10.1098/rspa.1974.0042